

Multi-track Geometry Prediction in Powder Fed Laser Additive Manufacturing Using Machine Learning

L. Botelho*, R. H. van Blitterswijk*, A. Khajepour*

* Automated Laser Fabrication Laboratory, Mechanical and Mechatronics Engineering,
University of Waterloo, Waterloo, Ontario N2L 3G1, Canada

Abstract

Laser additive manufacturing (LAM) allows for complex geometries to be fabricated without the limitations of conventional manufacturing. However, LAM is highly sensitive to small disturbances, resulting in variation in the geometry of the produced layer (clad). Therefore, in this research a monitoring algorithm is discussed with the capability of predicting the geometry of multiple tracks of added material. Though imaging can be used to measure the geometry of the melt pool during LAM, the appearance of the melt pool changes in multi-track processes due to the previous layers causing measurement errors. Hence, a machine learning algorithm may be able to accommodate for the changing melt pool appearance to improve accuracy. Images can be captured during LAM with visible-light and infrared sensors which may provide sufficient information for the geometry to be predicted. A convolutional neural network (CNN) can then use these images to estimate the geometry (height and width) during LAM processes.

Keywords: Laser Additive Manufacturing, Machine Learning, Convolutional Neural Network

Introduction

During laser additive manufacturing (LAM), the geometry of the added material (clad) is critical to monitor in real-time to ensure the final part has the correct dimensions. It has been shown that even in cases where constant process parameters were used, the height of subsequent layers can vary, which motivates the need for geometry monitoring [1]. However, the experimental setup of LAM machines may make it difficult to directly measure the geometry of the clad in real-time; therefore, different methods have been devised to approximate the geometry in real-time.

In many cases the geometry is monitored with cameras, where the clad is detected in captured images, then the clad height can be calculated from direct mathematical relationships as in [2, 3]. Other applications have used colinear imaging to predict the width, such as Hofman et al. in [4]. Some systems have also been used to monitor the height and width simultaneously, such as a U.S. patent by Suh which describes a methodology to monitor and control the clad height in laser cladding in real-time [5]. However, since the relationship between 3d geometry and the 2d image captured may be difficult to determine, some research has been devoted to utilizing machine learning (ML) to predict the geometry in real-time.

One approach for measuring the height in real-time was explored by Iravani et al. in which images of the melt pool were captured by three cameras positioned 120° apart

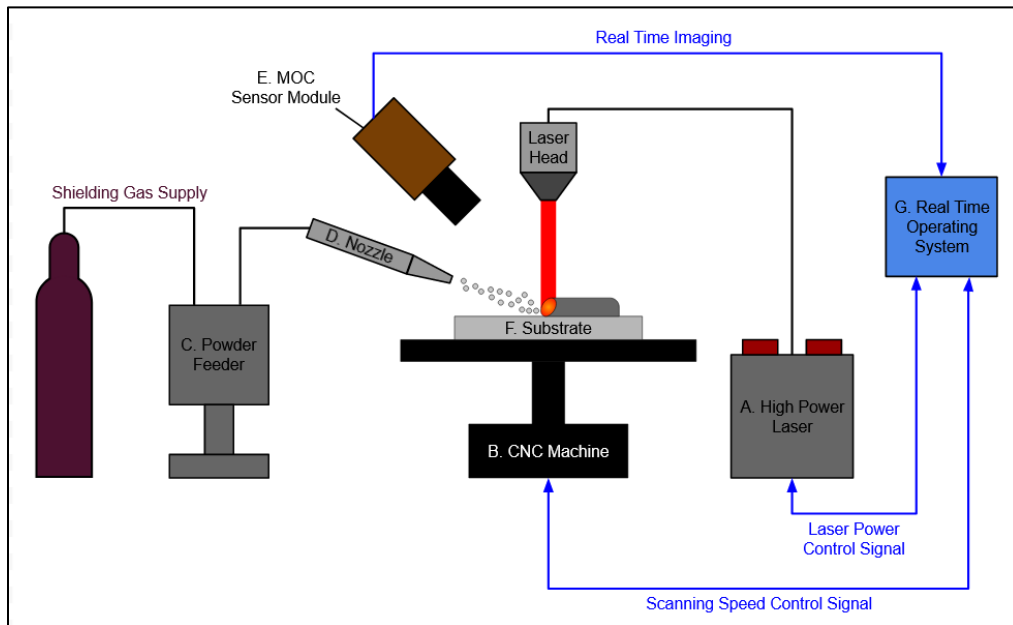
[6]. A recurrent neural network (RNN) was then able to predict the clad height with an average error of approximately 12%. Other research in ML has been applied to find a relationship between process parameters and geometry in additive manufacturing (AM) and arc welding to control the process parameters to compensate for geometry errors [7, 8, 9] Goncalves et al. applied a more complex CNN to establish a correlation between real-time vision images with process parameters and clad geometry [10]. Thus, ML has been applied to find relationships between the geometry, real-time images, and process parameters. However, most of the current research is limited to single-track geometry. One example of multi-track geometry monitoring was applied by Garmendia et al. in which a 3D scanner monitored the height after each set of layers [11]. However, since the height was measured between several layers this method is insufficient for real-time applications.

Since the view of the clad does not allow for the geometry to be measured directly and the potential that has been shown in applying ML to predict the geometry, this approach is further explored in this research. Moreover, most research is focused on single-track geometry prediction since previous tracks affect the appearance of later tracks the same geometry calculations often cannot be applied. However, this research focuses on multi-track experiments, which feature layers formed on top of one another with the same x and y coordinates and changes in the z-direction to compensate for the height of previous layers. Therefore, the goal of this research is to develop a CNN to predict the height and width of the clad during multi-track laser additive manufacturing in real-time using images captured by a vision camera and infrared camera. Training a CNN to solve this challenge removes the need to determine a direct relationship between the captured images and clad geometry which may differ based on the LAM system and materials used.

Experimental Setup

A schematic diagram of the experimental setup is shown in Figure 1. The experimental setup features a system to perform powder fed LAM to run experiments to create a dataset to train the proposed CNN. The main components of powder fed LAM are: (1) Substrate, the platform in which the part is built upon, relative motion between the laser head and the substrate allows for 3D geometry to be fabricated. The first layer of the part is bonded directly to the substrate, while later layers are bonded to the previous layers. (2) Powder nozzle, the powder nozzle is connected to a powder feeder which mixes the metal powder with inert gas and feeds the mixture to the path of the laser. The inert gas has secondary purposes to transporting the powder, the gas also inhibits the oxidation at the surface of the newly created clad and the gas also removes plasma from the melt pool area. (3) Laser, which is used to provide enough heat to melt the metal powder and enough of the substrate or previous layer to facilitate bonding. (4) The clad, a layer of additive material, which is formed when the melt pool solidifies, the geometry of which is determined by the tool path and other process parameters. All these components are shown in the schematic diagram below in Figure 1. The experimental setup also shows the Monitoring Optimization and Control MOC Sensor module, which is a device used to capture images of the process in real-time. In addition to the MOC

sensor, an operating system to record and control the critical process parameters such as the laser power and scanning speed.

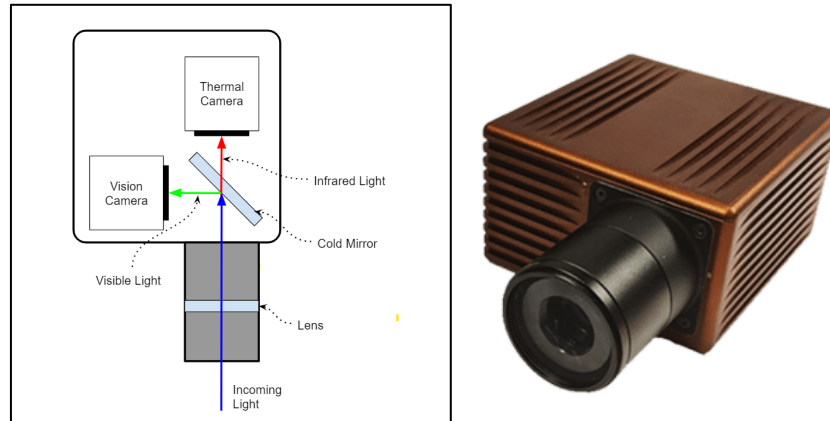


The main components of the experimental setup are:

- A. **High Power Laser** – provide energy to initiate the fusion of materials, the system features a laser with a diameter of 3mm and a Gaussian power distribution.
- B. **CNC Machine** – move the substrate to allow for geometry manipulation.
- C. **Powder Feeder** – add new material to the substrate during additive manufacturing.
- D. **Nozzle** – ensure the added material is placed in the correct location.
- E. **MOC Sensor Module** – provide visual information of the melt pool in real-time.
- F. **Substrate** – workpiece for the initial layer of powder to bond to during additive manufacturing.
- G. **Real-Time Control System** – control the process and integrate the other components.

MOC System

Real-time imaging of the clad is essential for geometry prediction to ensure the current state of the clad is known. Therefore, to accomplish this both infrared images and visible-light images are captured to observe the clad during the process. Allowing both sensors to have a similar field of view (FOV) ensures that the images can be directly compared and augments the data since we have multiple readings of the same state. Housing both sensors in the same enclosure also reduces the overall volume of the system and would require only one fixture to support the monitor. This motivated the design of the MOC system, which is shown in Figure 2. This design features a single lens, allowing both sensors to have a similar FOV; however, the cold mirror allows the light to be split, so the correct wavelength is input to the corresponding sensor. With this optical setup, both infrared and visible-light images can be taken of the process in real-time.



Dataset

To create a CNN a dataset must be created which includes the desired inputs to the system and the correct outputs. For this research, the desired inputs of the system are infrared images, visible-light images, scanning speed, and laser power. Using these inputs, the CNN was trained to estimate the clad height and clad width. To create the dataset, 6 experiments were conducted in total, which are outlined in Table 1. Each experiment features 5 layers of a single 80mm track with a 0.5mm increase in the z-direction between each layer. A fixture was used to secure the substrate to ensure the tracks are aligned directly above the previous layer. Figure 3 shows the clad formed in experiment 1 to demonstrate the print path of the experiments.

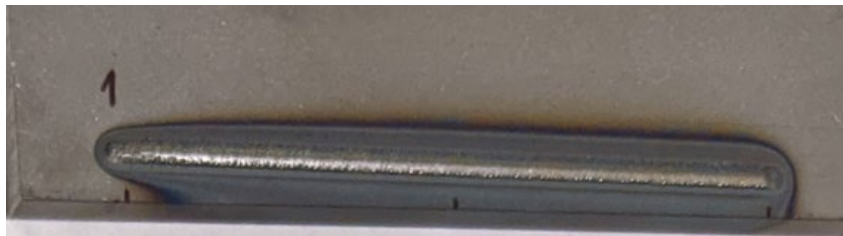


Figure 3: Clad created from first layer of experiment 1

During these experiments, images were captured using both camera sensors, and the process parameters, laser power, and scanning speed, were recorded by the system. This data was then used to form the input section of the dataset.

Table 1: Details of experiments used to create the dataset used for training, testing, and validating the CNN

Experiment Number	Laser Power (W)	Scanning Speed (mm/min)
1	950	100
2	950	100
3	950	120
4	950	80

5	850	100
6	1050	100

Of the experiments shown in Table 1, experiments 2-6 were used to create a dataset which was shuffled to form the training, validation, and test subsets for training and validating the CNN. Experiment 1 was used to demonstrate the performance of the CNN against a dataset that was not involved in training. Experiments 1 and 2 have the same process parameters to ensure that the data from experiment 1 was not seen by the CNN, but similar data was used in training.

To create the outputs for the dataset, the true geometry must be known, so the CNN is trained with the correct information. The height and width of the clad are measured after the process using macro-imaging, which allows a zoomed-in image of the clad to be taken. This image can then be segmented to differentiate the clad from the background and knowing the scale of the image the geometry can be extracted. The true geometry was measured for each layer, and a fixture on the CNC ensured that the substrate would have the same starting location for all subsequent layers. With the true geometry measured, the framerate of the images being recorded in real-time can be used to align the real-time captured data to the true geometry measurements.

Pre-processing

With the dataset created with real-time measurements functioning as the inputs and true measurements as the outputs some pre-processing was conducted to improve the efficiency of the algorithm. Since the clad is only visible in a section of the images it is reasonable to crop the images to remove the background information. Removing this background information also reduces the size of the dataset, which improves computational efficiency without sacrificing performance since that part of the image is irrelevant.

To reduce the size of the images the procedure shown in Figure 4: Series of pre-processing steps conducted on the vision images was followed. First, the image was thresholded to determine the approximate location of the clad, which was assumed to be the largest observable shape after thresholding. Based on this location, the image could be cropped to a reduced size of 254×254 pixels. Finally, to further reduce the size, the images were scaled to 128×128 pixels.

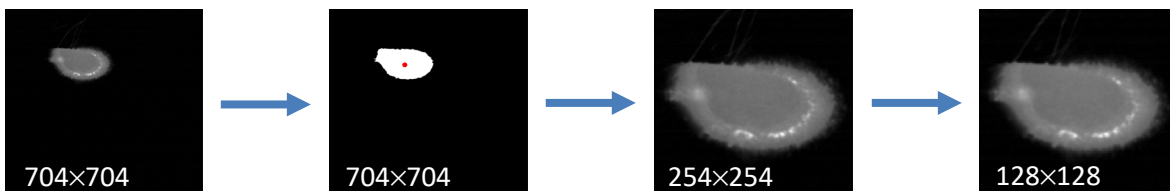


Figure 4: Series of pre-processing steps conducted on the vision images.

The same procedure outlined in was used to reduce the size of the infrared images, except for scaling the images, since these images were a lower resolution to begin with. Therefore, once the location of the clad was approximated, the images were cropped

directly into 128×128 . Once the completed dataset was created the data was shuffled and split into 60% - training, 20% - validation, and 20% - testing. These subsets of the data are used to train and test the CNN.

Convolutional Neural Network

As stated in the introduction, the goal of this research is to develop a computationally efficient machine learning algorithm to accurately predict the clad geometry, by using real-time vision and infrared images and the process inputs during multi-track LAM. Therefore, a CNN is developed that predicts the clad geometry using vision and infrared images, and process inputs. The developed CNN predicts the clad width and clad height from 128×128 vision and infrared images and process inputs of a laser cladding process. The CNN is trained to minimize the mean squared error (MSE) between the predicted clad geometry and the actual clad geometry. The architecture of the CNN is shown in Figure 5 which uses seven different operators.

This CNN architecture is made of two deep network branches, in which the infrared images are the input for the first branch and the vision images are the input of the second branch. Each branch consists of four blocks of two conv layers with batch normalization and relu activation, and a maxpooling layer. After these four blocks, the branch output is flattened into a 1-dimensional array. After that, both branches are combined with the process laser power, process scanning speed, and the layer number. This combined layer is fed through two fully connected layers followed by a linear activation. The linear activation outputs the prediction of the clad width and clad height.

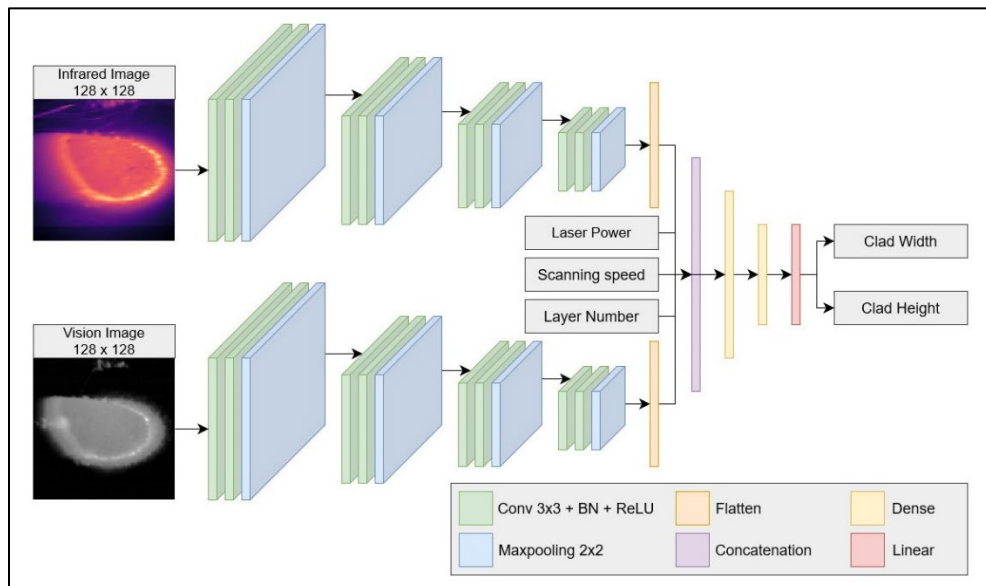


Figure 5: Convolutional neural network architecture used to predict the clad with and clad height.

Loss function

One of the important components of the CNN is the loss function. The loss function calculates the prediction error, and this prediction error is used to update the weights of the CNN. Because the developed CNN is used for regression, the mean squared error (MSE) is used as a loss function. The MSE is the mean of the squared differences between the predicted and actual values, which is calculated by:

$$MSE = \frac{1}{p} \sum_{i=1}^p (\hat{y}^i - y^i)^2$$

where p is the amount of data samples; \hat{y} is a vector with the predicted clad width and clad height; and y is a vector with the actual clad width and clad height.

To evaluate the performance of the developed CNN quantitatively, the mean absolute percentage error (MAPE) is calculated. The MAPE is a measure of average error between the LAM process measurements and CNN predictions. In addition, the MAPE is easy to understand because the error is calculated in terms of percentages. The MAPE is calculated by:

$$MAPE = \frac{1}{p} \sum_{i=1}^p \left| \frac{\hat{y}^i - y^i}{\hat{y}^i} \right|$$

where again p is the amount of data samples; \hat{y} is a vector with the predicted clad width and clad height; and y is a vector with the actual clad width and clad height.

Results

After training the CNN for 200 epochs, the performance of the CNN is analyzed on the original dataset. The developed CNN resulted in an MSE of less than 0.0006 and MAPE of less than 2.05%. These values show that the CNN established a highly accurate correlation between the images with process inputs and the clad dimensions. To further analyze the overall accuracy of the CNN on the original dataset, the clad width and clad height predictions, are compared to the actual clad width and clad height values. This comparison is shown in Figure 6 and shows that the CNN fits the data well. The differences between the actual values, during multi-track LAM, and the CNN predictions are very small. The CNN features an average computational time of approximately 0.037 seconds per timestep, allowing for the geometry to be predicted at a frequency of 27Hz.

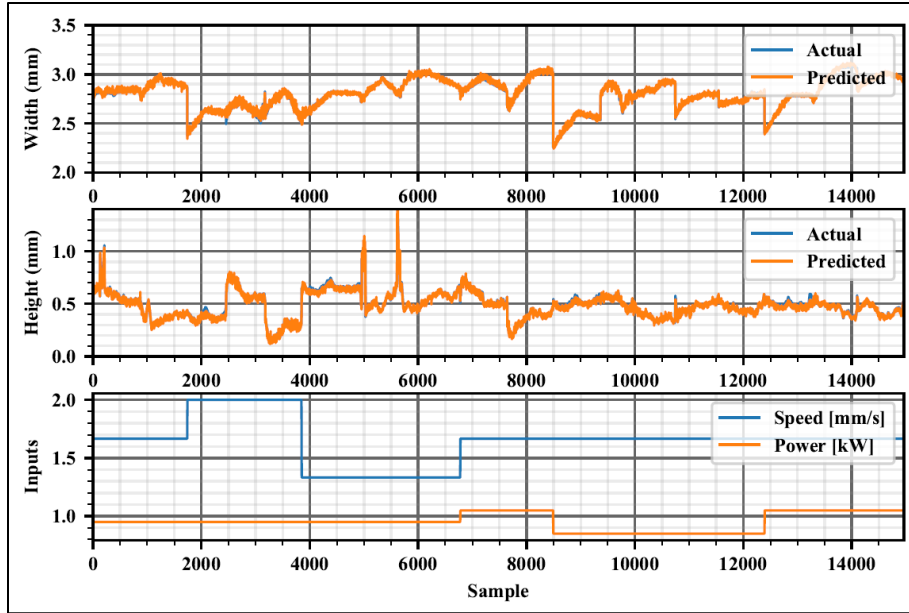


Figure 6: CNN predictions compared with the actual measurements when using the original dataset. Note that for the combined data set comprised on the training, validation, and test sets the predictions are sufficient such that the actual measurements are barely visible on this graph.

Figure 7, which compared the data (blue dots) to the regression line (black). As shown in this figure, the CNN fits the data well. However, this figure shows that there are a few outliers, which could be caused by noise in the data or overfitting of the CNN.

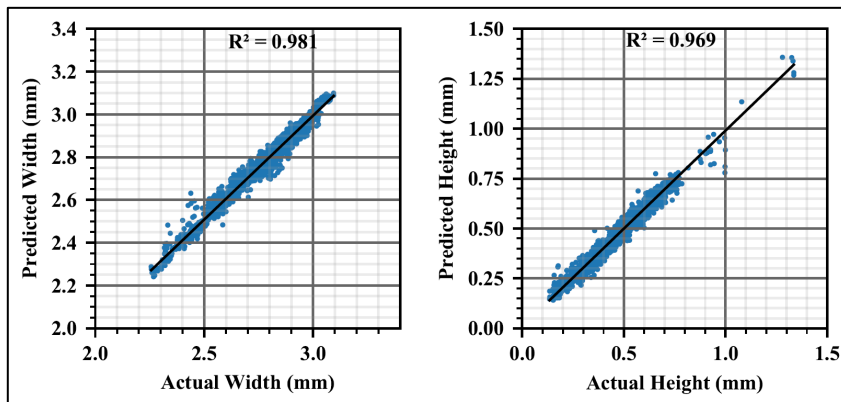
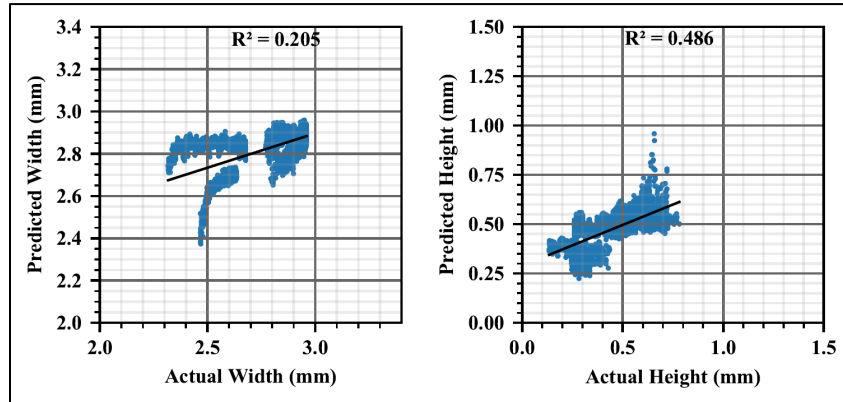


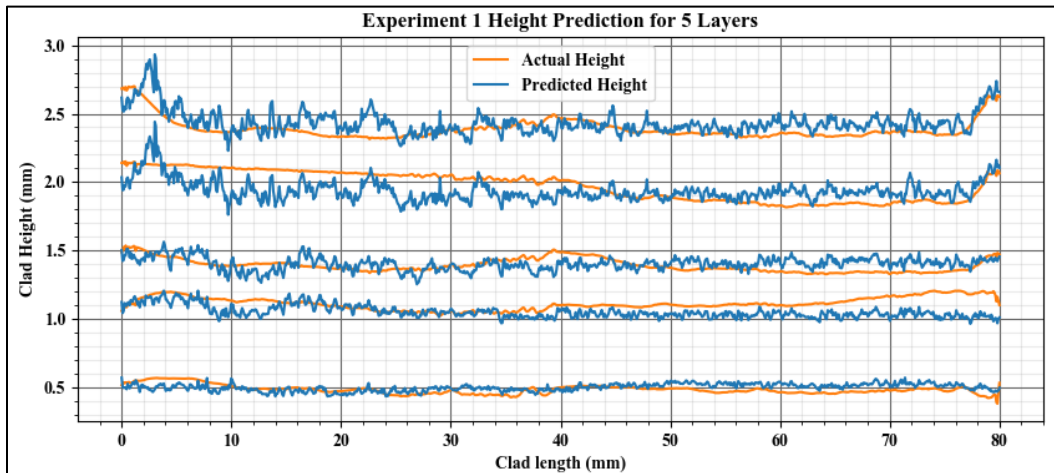
Figure 7: Coefficient of determination between the actual and predicted geometry, generated from the test set.

Table 1 was not used in the training, validation, or test sets and therefore demonstrates the performance of the CNN

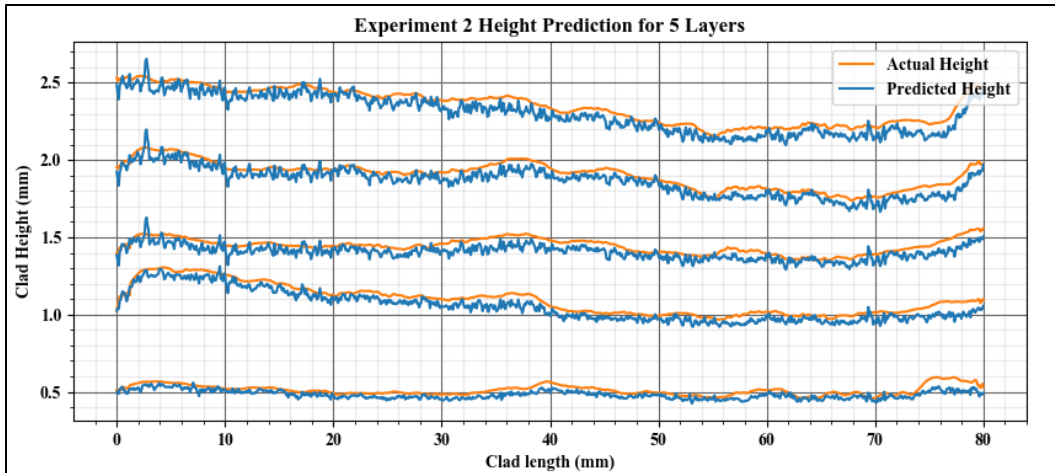
against unseen data. When only considering experiment 1, the MSE corresponded to approximately 0.016, while the MAPE was approximately 12.41%. This performance can also be quantified in Figure 8, where the calculated clad width R^2 value is 0.205 and the calculated clad height R^2 value is 0.486, indicating relatively poor performance.



The graph shown in Figure 9 features the height predictions of all 5 layers added to show the accumulated error. This figure also better visualizes the performance of the CNN against the unseen dataset.



Demonstrating the cumulative height predictions of experiment 2, which features the same process parameters, shows even less accumulation of error, as seen in Figure 10.



Conclusion

In this research, a computational efficient CNN was developed for the purpose of real-time multi-track clad geometry prediction. The developed CNN architecture is trained with a dataset which captured the basic modes of the laser cladding process. This CNN can easily be extended to different scenarios by adding more training data from a wider range of experiments and re-training the network. The results demonstrated that the developed CNN is accurate and computationally efficient for the prediction of the clad geometry during multi-track LAM. The prediction error is below 2.05% for the training, validation and testing set and below 12.5% for the unseen dataset with an average prediction time of approximately 0.037 seconds. Though the CNN featured impressive performance against the test set, where some data was used for training, the performance was relatively poor with unseen data. However, future improvements to the network and increasing the training set may improve the results of unseen data to resemble the test set results more closely.

The good performance of the test set, which features data from the same experiments as the training set, indicates that with improved training the CNN may predict unseen data with similar performance to the test set. The CNN does not assume any prior knowledge of the clad which allows for training to cover multiple different manufacturing processes and materials. Thus, the high accuracy, computational efficiency, and flexibility of this CNN makes it suitable for closed-loop control of the clad geometry. In addition, this network may even be applicable to a wider group of manufacturing techniques.

Future work

To advance the primary work done in this research and to improve the performance and generality of the developed convolutional neural network, the network can be retrained with a dataset that uses a wider range of process inputs, substrate and powder materials, camera settings and positions, and manufacturing techniques. Though experiments 1 and 2 featured the same process parameters, the CNN only achieved a MAPE of when predicting the geometry for experiment 1. Therefore, there may be other

process disturbances that were not initially considered which differentiate experiment 1 and 2 which caused the difference in results. Adding more process parameters as an input to the CNN would provide more information that may be relevant in predicting the geometry. Other parameters that can be added to the prediction include, powder feed rate, powder size, gas flow rate, laser diameter, and other features, though these features must be statistically analyzed to determine which are significant. Changing the architecture of the model into a recurrent neural network (RNN) may also improve the results by reducing the influence of outliers and noise in the system, wince RNNs consider data from previous timesteps. Applying these improvements to the CNN would allow it to be used in a closed-loop control system to demonstrate the potential for better quality LAM parts. Finally, the network may also be expanded to include predictions for microstructure and porosity.

Acknowledgment

The authors would like to acknowledge the financial support of the Natural Sciences and Engineering Research Council of Canada.

References

- [1] H. El Cheikh, B. Courant, S. Branchu, X. Huang, J.-Y. Hascoet and R. Guillen, "Direct Laser Fabrication process with coaxial powder projection of 316L steel. Geometrical characteristics and microstructure characterization of wall structures," *Optics and Lasers in Engineering*, vol. 50, pp. 1779-1784, 2012.
- [2] L. Song, V. Bagavath-Singhm, B. Dutta and J. Mazu, "Control of melt pool temperature and deposition height during direct metal deposition process," *International Journal of Advanced Manufacturing Technology*, vol. 58, pp. 247-256, 2011.
- [3] T. A. Davis and Y. C. Shin, "Vision based clad height measurement," *Machine Vision and Applications*, vol. 22, pp. 129-136, 2010.

- [4] J. T. Hofman, B. Pathirai, J. van Dijk, D. F. de Lange and J. Meijer, "A camera based feedback control strategy for the laser cladding process," *Journal of Materials Processing Technology*, vol. 212, no. 11, pp. 2455-2462, 2012.
- [5] J. Suh, "Method and System for Real-Time Monitoring and Controlling Height of Deposit by Using Image Photographing and Image Processing Technology in Laser Cladding and Laser-Aided Direct Metal Manufacturing Process". United States of America Patent 7423236, 2008.
- [6] M. Iravani-Tabrizipour and E. Toyserkani, "An image based feature tracking algorithm for real-time measurement of clad height," *Machine Vision and Applications*, vol. 18, pp. 343-354, 2007.
- [7] H. Liu, X. Qin, S. Huang, L. Jin, Y. Wang and K. Lei, "Geometry Characteristics Prediction of Single Track Cladding Deposited by High Power Diode Laser Based on Genetic Algorithm and Neural Network," *International Journal of Precision Engineering and Manufacturing*, vol. 19, pp. 1061-1070, 2018.
- [8] F. Caiazzo and A. Caggiano, "Laser Direct Metal Deposition of 2024 Al Alloy: Trace Geometry Prediction via Machine Learning," *Materials*, vol. 11, no. 3, p. 444, 2018.
- [9] J. Xiong, G. Zhang, J. Hu and L. Wu, "Bead geometry prediction for robotic GMAW-based rapid manufacturing through a neural network and a second-order regression analysis," *Journal of Intelligent Manufacturing*, vol. 25, pp. 157-163, 2014.
- [10] D. A. Goncalves, M. R. Stemmer and M. Pereira, "A convolutional neural network approach on bead geometry estimation for a laser cladding system," *The International Journal of Advanced Manufacturing Technology*, vol. 106, no. 5, pp. 1-11, 2020.
- [11] I. Garmendia, J. Leunda, J. Pujana and A. Lamikz, "In-process height control during laser metal deposition based on structured 3D scanning," in *19th CIRP Conference on Electro Physical and Chemical Machining*, Bilbao, Spain, 2018.